Supplementary Information

In silico Analysis of SOD1 Aggregation Inhibition Modes of Tertiary Amine Pyrazolone and Pyrano Coumarin Ferulate as ALS drug candidates

Aziza Rahman, Bondeepa Saikia, and Anupual Baruah*

Department of Chemistry, Dibrugarh University, Dibrugarh, Assam, India, 786004

The following are the reason for selection of one conformation to be considered for MD simulation from five docked conformations:

- For TAP at dimeric interface: second lowest binding energy; best CF and MBE of the cluster. (The conformation having lowest binding energy has a poor CF of the cluster)

- For TAP at W32 binding site: lowest binding energy; best CF and second best MBE of the cluster

- For TAP at UMP binding site: lowest binding energy; best CF and second best MBE of the cluster

- For PCF at dimeric interface cavity: lowest binding energy; best CF and second best MBE of the cluster

- For PCF at W32 binding site: second lowest binding energy; good CF with one of the best MBE. (The conformation having the lowest binding energy has poor MBE of the cluster, so it is not considered)

- For PCF at UMP binding site: second lowest binding energy; second best CF and best MBE of the cluster. (The conformation having lowest binding energy has poor CF of the cluster)
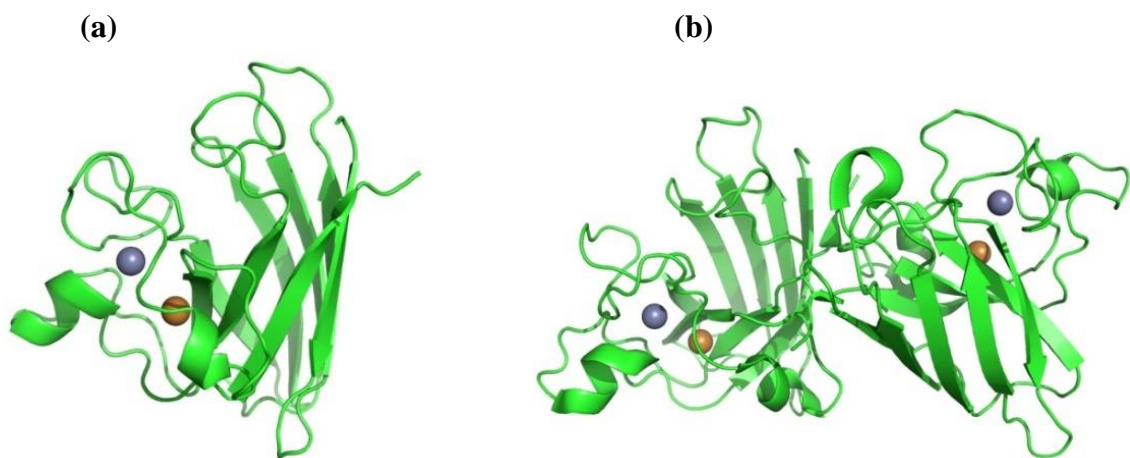
Figure S1: G93A mutant **(a)** monomer **(b)** dimer
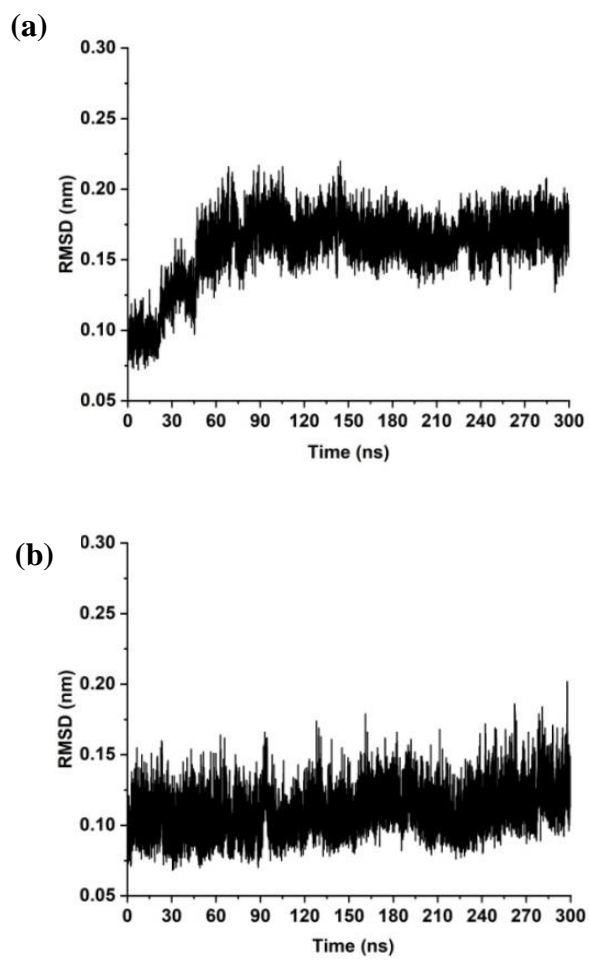
Figure S2: RMSD plots of the **(a)** MT-SOD1 monomer **(b)** MT-SOD1 dimer
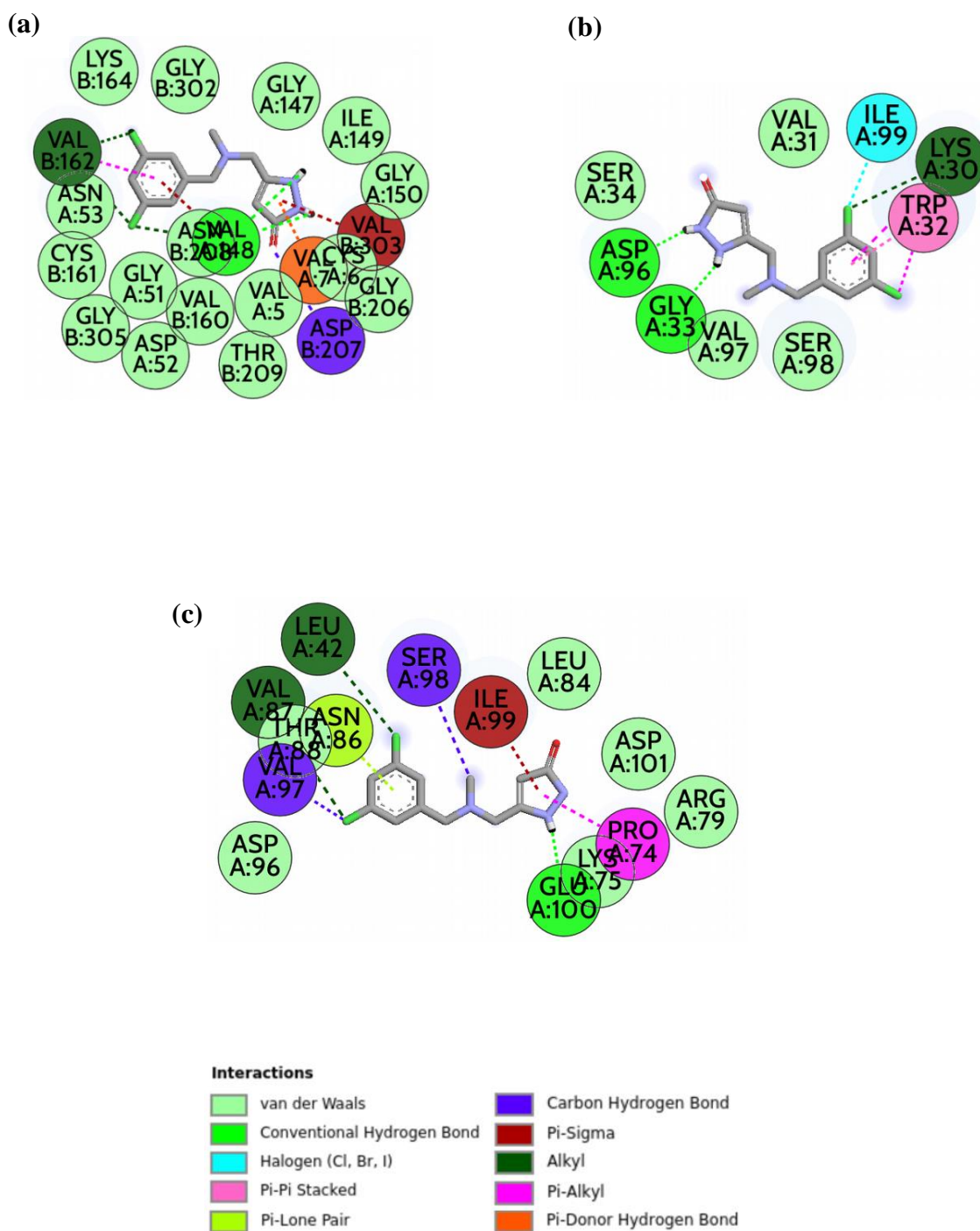
Figure S3: Various interactions shown by the best-docked conformers selected for TAP binding to MT-SOD1 at **(a)** dimeric interface cavity **(b)** W32 binding site **(c)** UMP binding site

(a)

(b)

(c)

Interactions

▢	van der Waals	▮	Carbon Hydrogen Bond
▮	Conventional Hydrogen Bond	▮	Pi-Sigma
▮	Halogen (Cl, Br, I)	▮	Alkyl
▮	Pi-Pi Stacked	▮	Pi-Alkyl
▮	Pi-Lone Pair	▮	Pi-Donor Hydrogen Bond
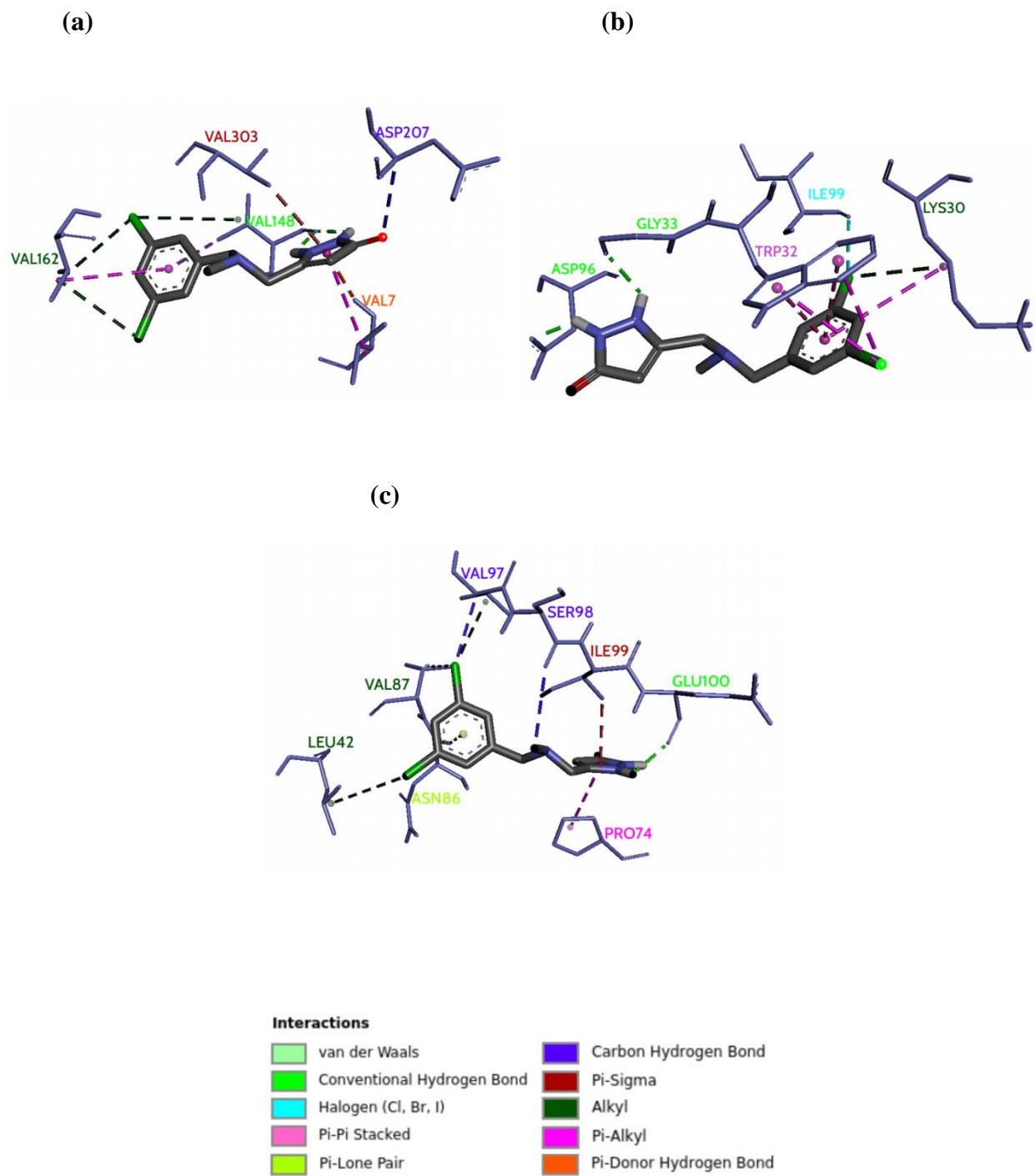
Figure S4: 3D representation of the various interactions shown by the best-docked conformers selected for TAP binding to MT-SOD1 at **(a)** dimeric interface cavity **(b)** W32 binding site **(c)** UMP binding site

Binding site	Interactions									
	Van der waals	Convent ional H-bond	Carbon H-bond	Alkyl	Pi-Alkyl	Pi-Dono r H-bond	Pi-Sigma	Pi-Pi Stacke d	Pi-Lone Pair	Halogen (Cl,Br,I)
At DI	Val5, Cys6, Gly51, Asp52, Asn53, Gly147, Ile149, Gly150, Val160, Cys161, Lys164, Gly206, Asn208, Thr209, Gly302, Gly305	Val148	Asp207	Val148, Val162,	Val7, Val162	Val7	Val148, Val303	-	-	-
At W32	Val31, Ser34, Val97, Ser98	Asp96, Gly33	-	Lys30	Lys30, Trp32	-	-	Trp32	-	Ile99
At UMP	Lys75, Arg79, Leu84, Thr88, Asp96, Asp101	Glu100		Leu42, Val87, Val97	Pro74		Ile99	-	Asn86	-

Table S1: Various interactions shown by the best-docked conformers selected for TAP binding to MT-SOD1 at three different binding sites of SOD1
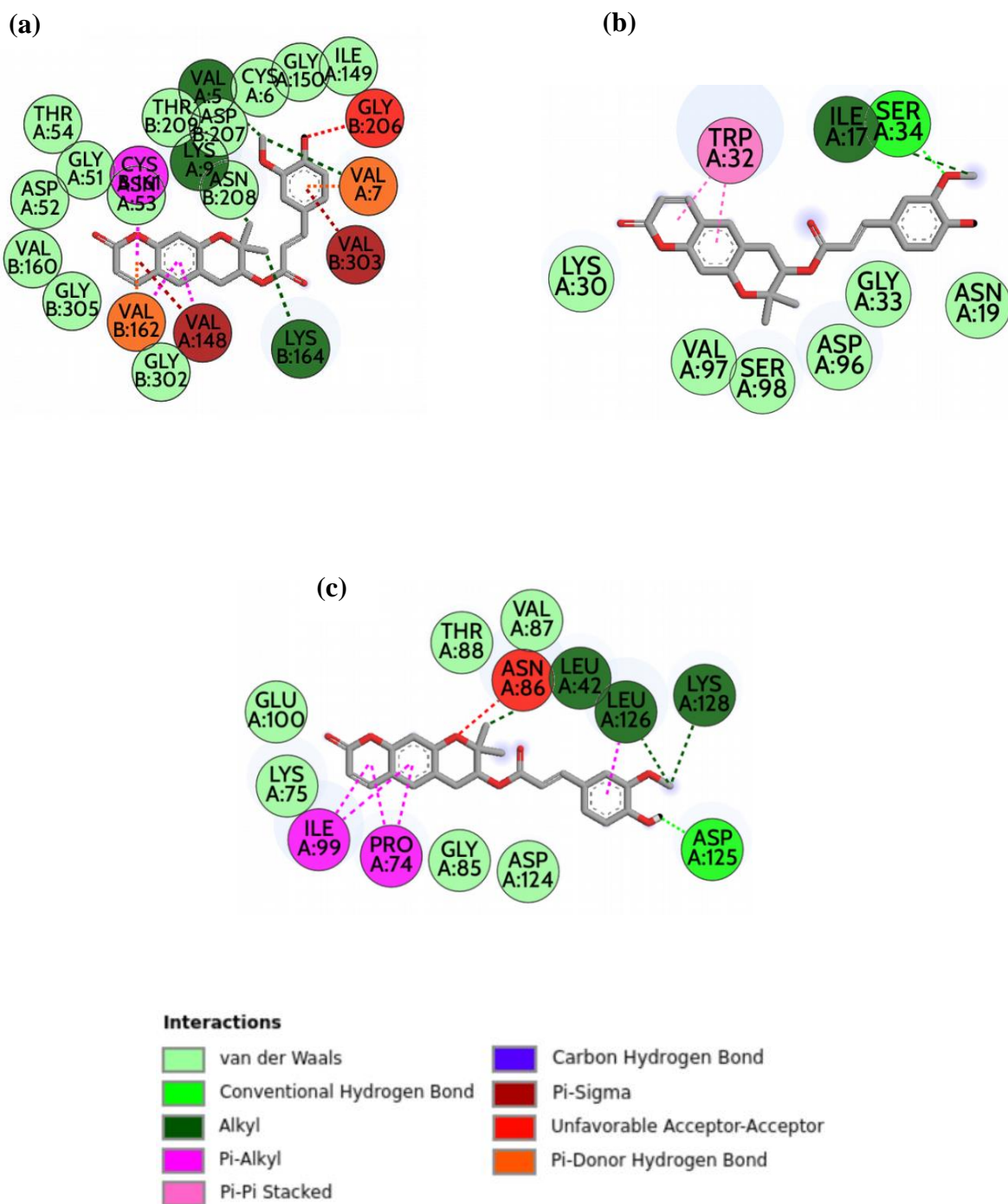
Figure S5: Various interactions shown by the best-docked conformers selected for PCF binding to MT-SOD1 at **(a)** dimeric interface cavity **(b)** W32 binding site **(c)** UMP binding site
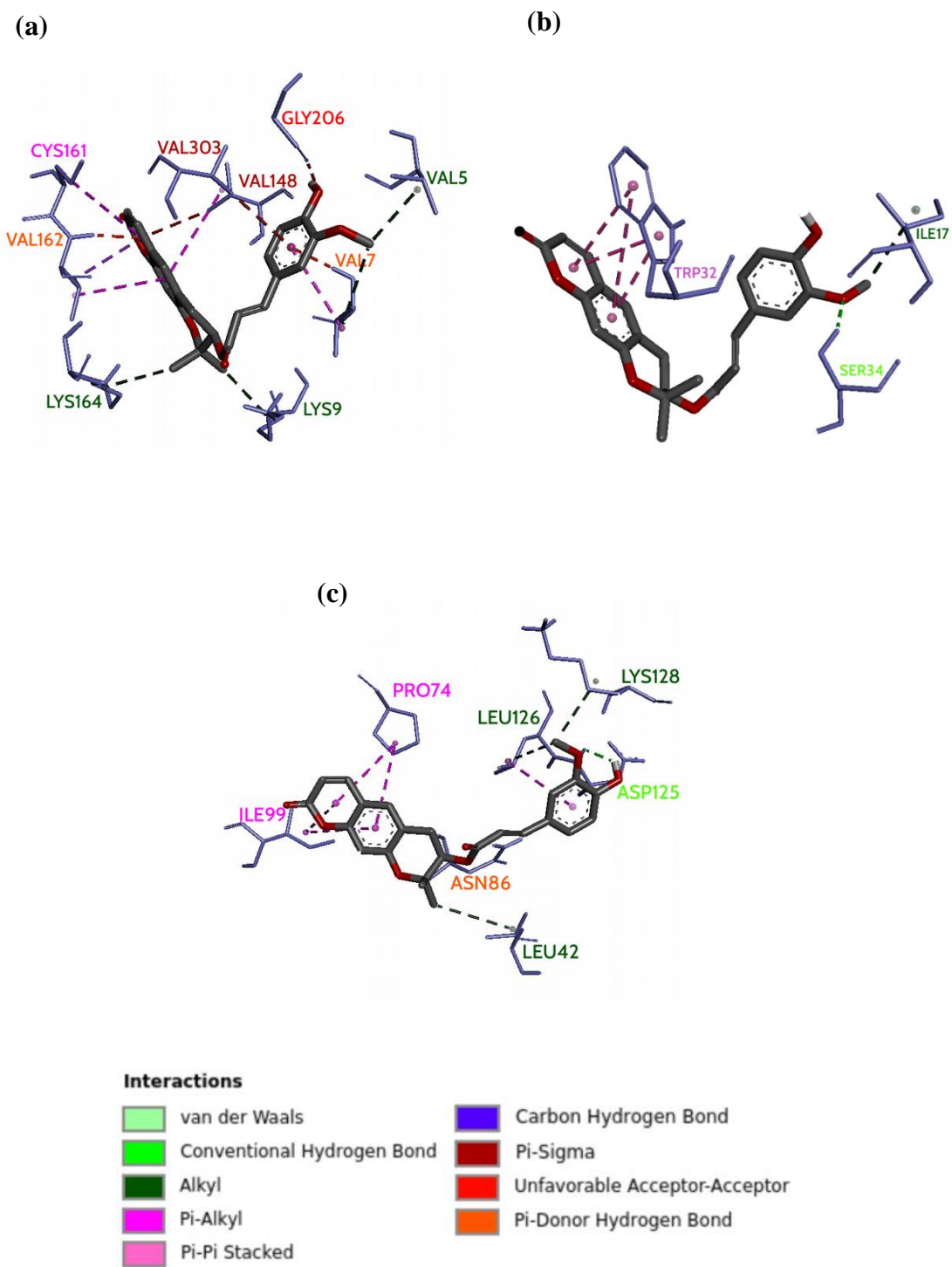
Figure S6: 3D representation of various interactions shown by the best-docked conformers selected for PCF binding to MT-SOD1 at **(a)** dimeric interface cavity **(b)** W32 binding site **(c)** UMP binding site

Binding site	Interactions								
	Van der waals	Conventional H-bond	Carbon H-bond	Alkyl	Pi-Alkyl	Pi-Donor H-bond	Pi-Sigma	Pi-Pi Stacked	Unfavourable Acceptor-Acceptor
At DI	Cys6, Gly51, Asp52, Asn53, Thr54, Ile149, Gly150, Val160, Asp207, Asn208, Thr209, Gly302, Gly305	-	-	Val5, Lys9, Lys164	Val7, Val148, Cys161, Val162	Val7, Val162	Val148, Val162, Val303	-	Gly206
At W32	Asn19, Lys30, Gly33, Asp96, Val97, Ser98	Ser34		Ile17	-	-	-	Trp32	-
At UMP	Lys75, Gly85, Val87, Thr88, Glu100, Asp124	Asp125	-	Leu42, Leu126, Lys128	Pro74, Ile99, Leu126	-	-	-	Asn86

Table S2: Various interactions shown by the best-docked conformers selected for PCF binding to MT-SOD1 at three different binding sites of SOD1
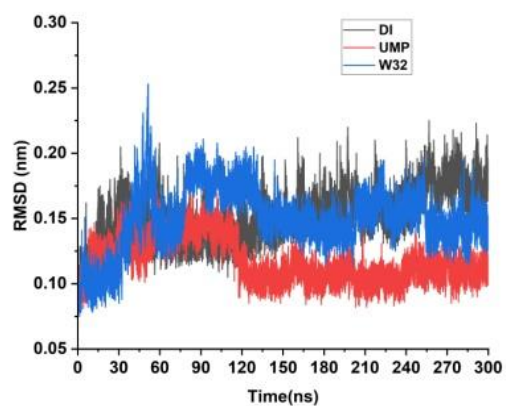
Figure S7: RMSD plot of the MT-SOD1-TAP system

(a)

(b)

(c)
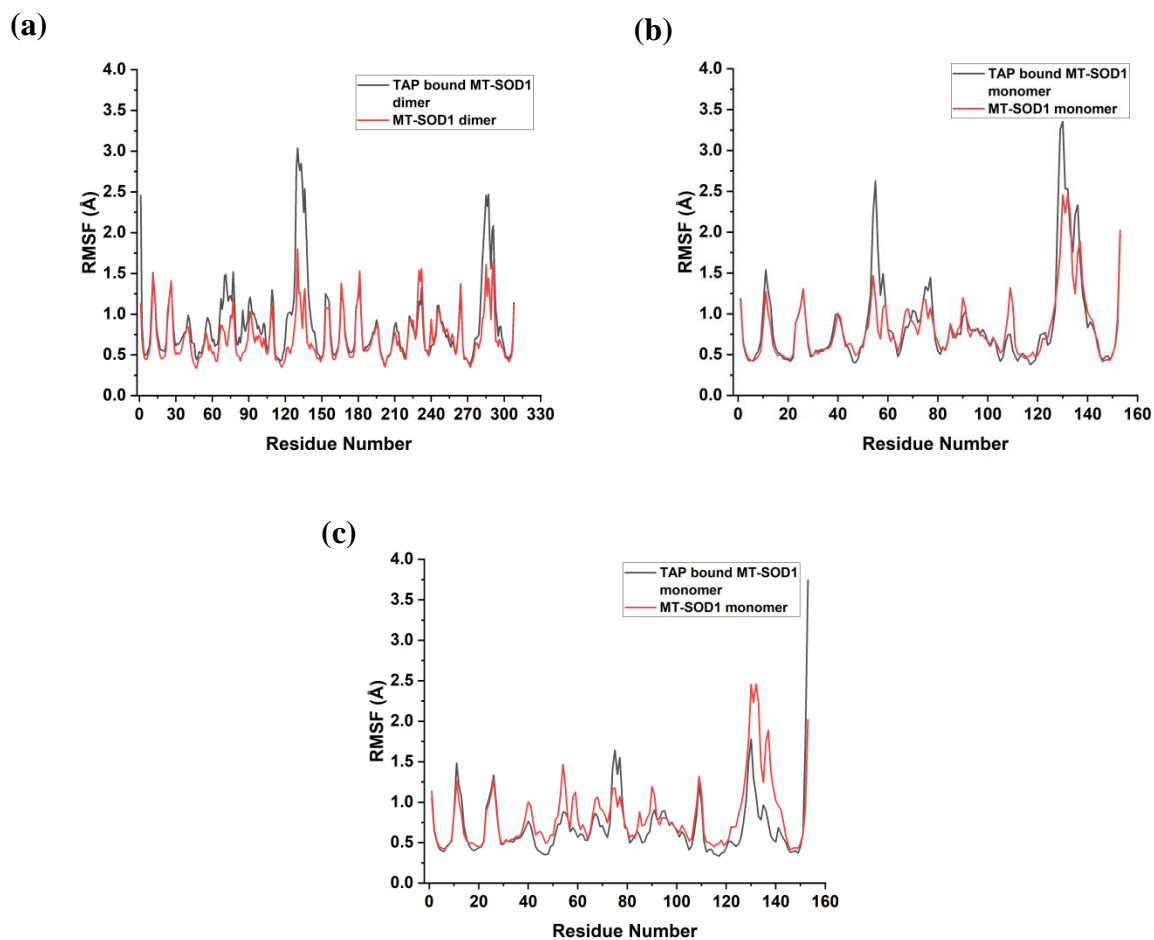
Figure S8: Plot depicting residual flexibility of the residues for TAP binding to MT-SOD1 at (a) dimeric interface cavity (b) W32 binding site **(c)** UMP binding site
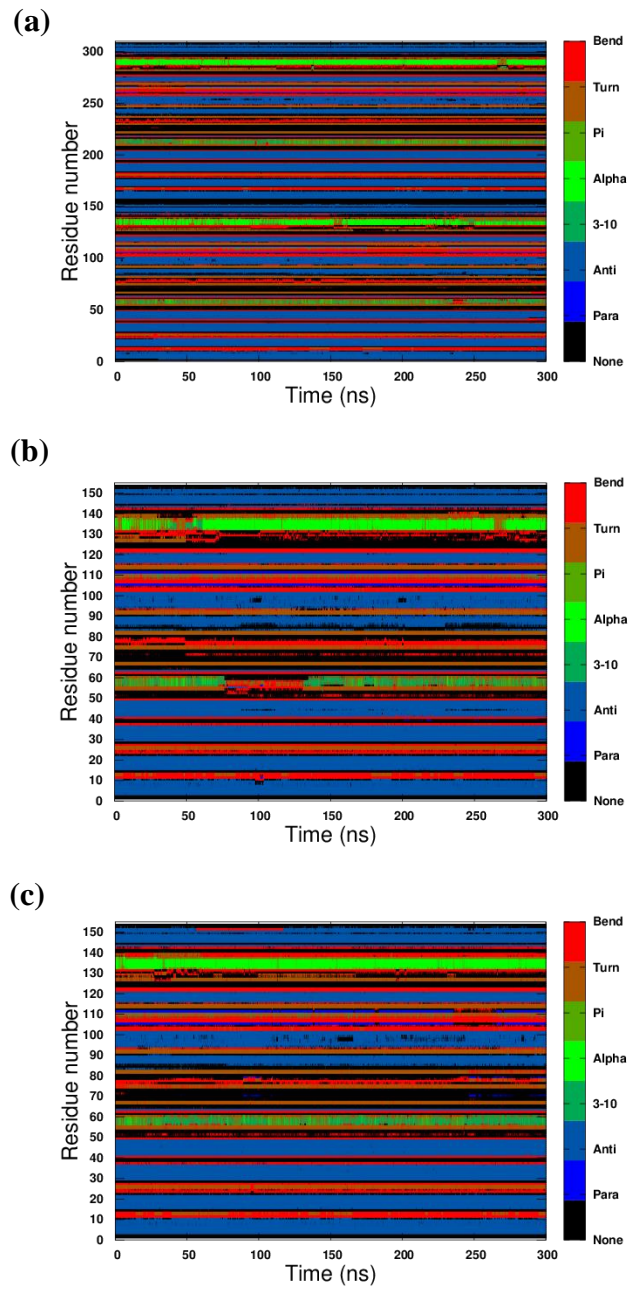
Figure S9: Secondary structure propensity analysis of the MD trajectories for TAP binding to MT-SOD1 at (a) dimeric interface cavity (b) W32 binding site **(c)** UMP binding site
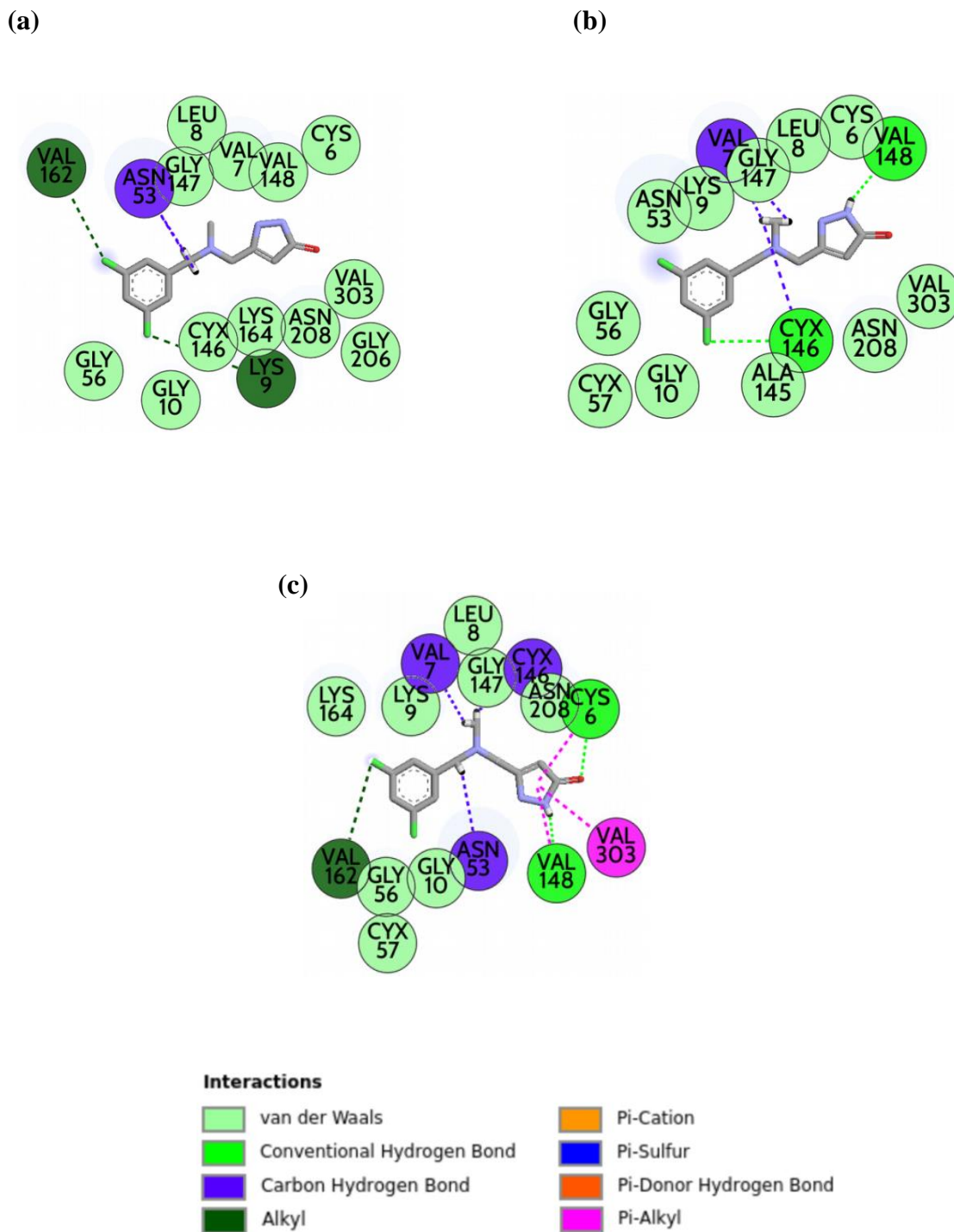
Figure S10: Snapshots of TAP bound to MT-SOD1 at the dimeric interface cavity of SOD1 at (a) 150 ns (b) 200 ns (c) 250 ns of MD simulation
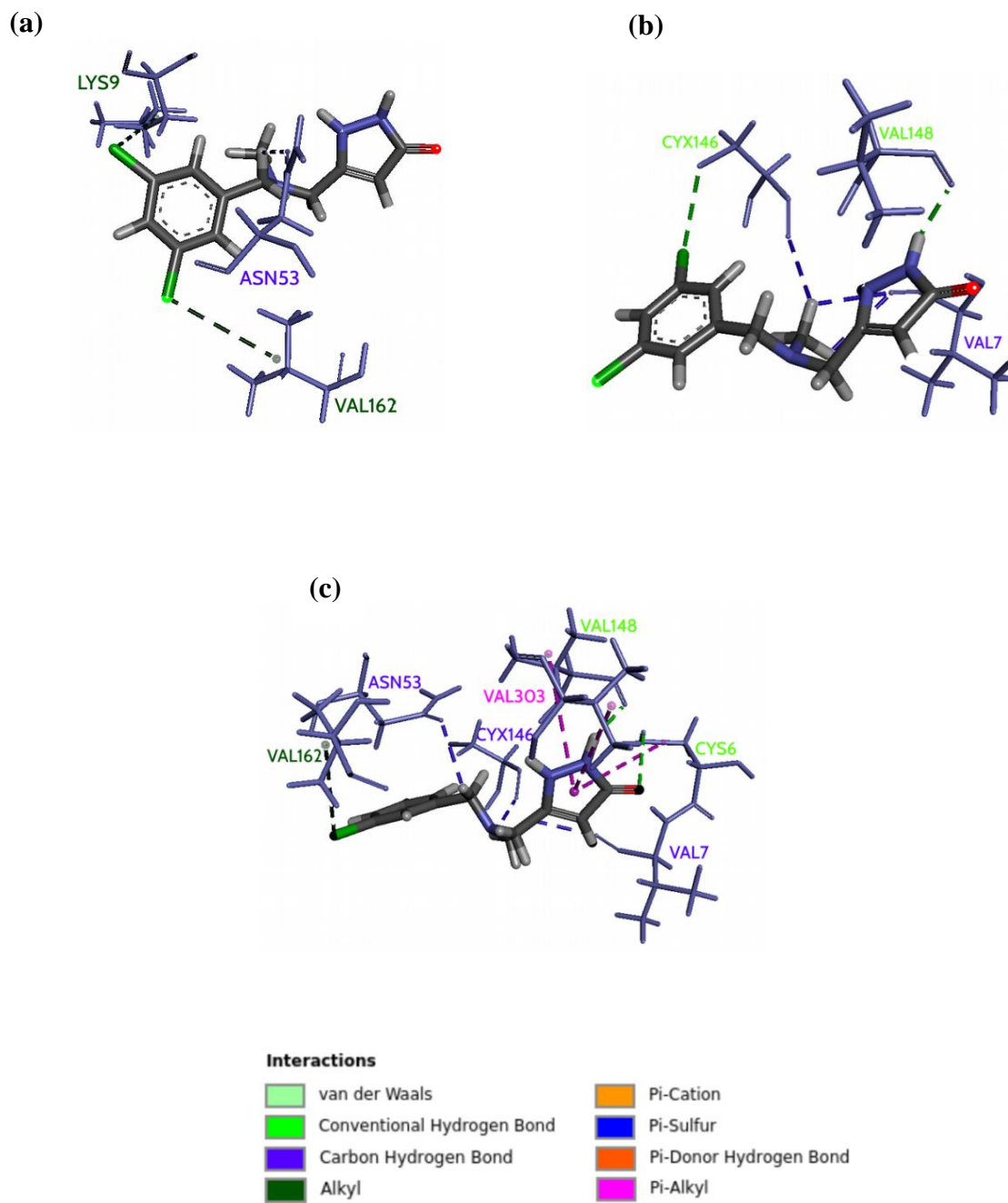
Figure S11: 3D representation of protein-ligand interactions shown by TAP bound to MT-SOD1 at the dimeric interface cavity of SOD1 at (a) 150 ns (b) 200 ns (c) 250 ns of MD simulation

Time	Interactions							
	Van der waals	Conventional H-bond	Carbon H-bond	Alkyl	Pi-Alkyl	Pi-Cation	Pi-Donor H-bond	Pi-Sulfur
100 ns	Val7, Gly10, Gly56, Cyx57, Cyx146, Val148, Val162, Lys164, Asn208, Val303	Cys6	Asn53, Gly147	Lys9	Lys9	-	-	-
150 ns	Cys6, Val7, Leu8, Gly10, Gly56, Cyx146, Gly147, Val148, Lys164, Gly206, Asn208, Val303	-	Asn53	Lys9, Val162	-	-	-	-
200 ns	Cys6, Leu8, Lys9, Gly10, Asn53, Gly56, Cyx57, Ala145, Gly147, Asn208, Val303	Cys146, Val148	Val7, Cyx146	-	-	-	-	-
250 ns	Leu8, Lys9, Gly10, Gly56, Cyx57, Gly147, Lys164, Asn208	Cys6, Val148	Val7, Asn53, Cyx146	Val162	Cys6, Val148, Val303	-	-	-
300 ns	Val7, Lys9, Gly56, Cyx57, Gly147, Asn208, Gly302	Cys6, Cyx146, Val148	Asn53, Lys164	Val162, Lys164	Val148, Val162, Val303	Lys164	Val148	Cyx146

Table S3: Various interactions shown by the TAP bound to MT-SOD1 at the dimeric interface cavity of SOD1
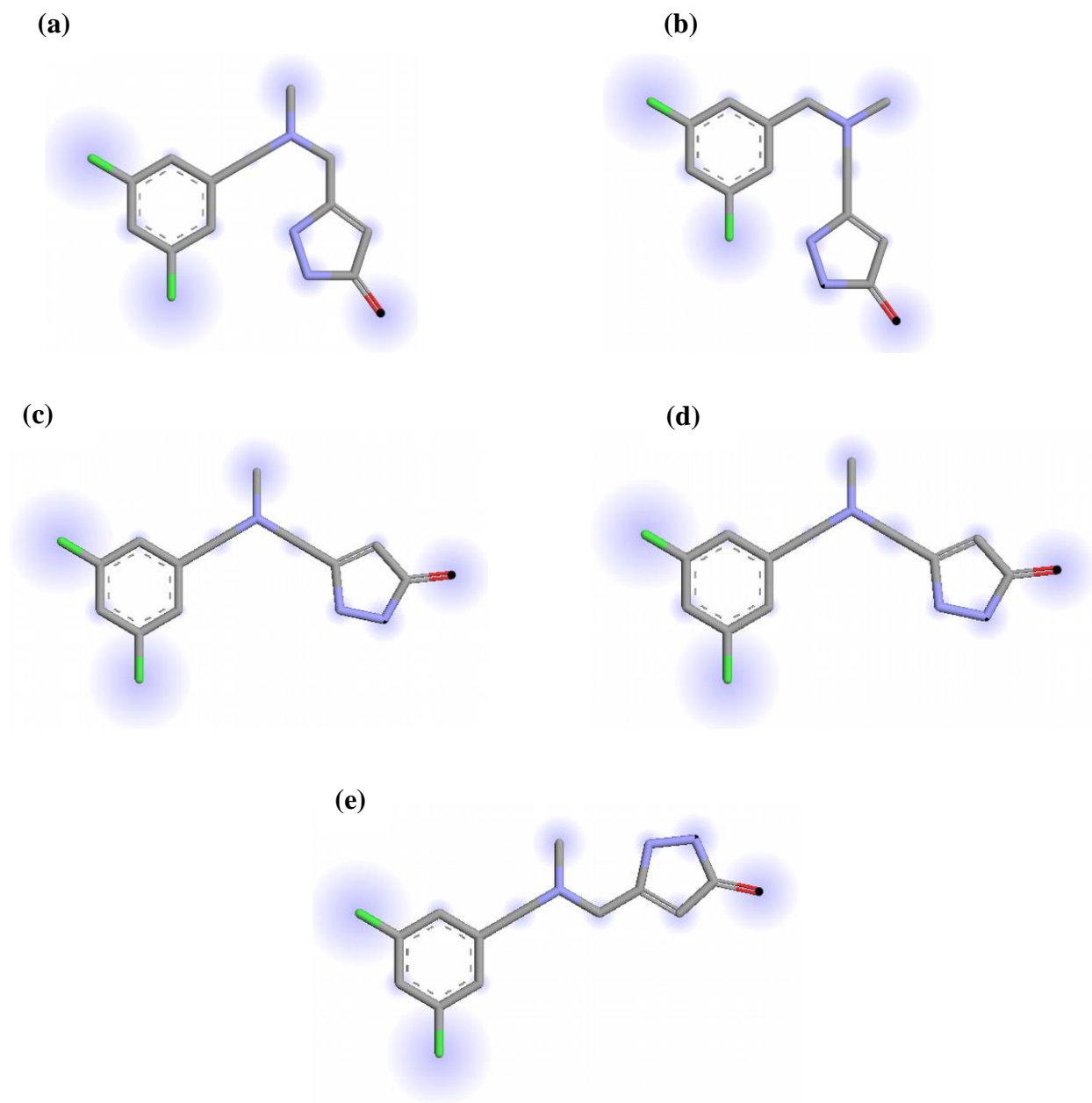
Figure S12: Snapshots of TAP bound to MT-SOD1 at the W32 binding site of SOD1 at (a) 100 ns (b) 150 ns (c) 200 ns (d) 250 ns (e) 300 ns of MD simulation
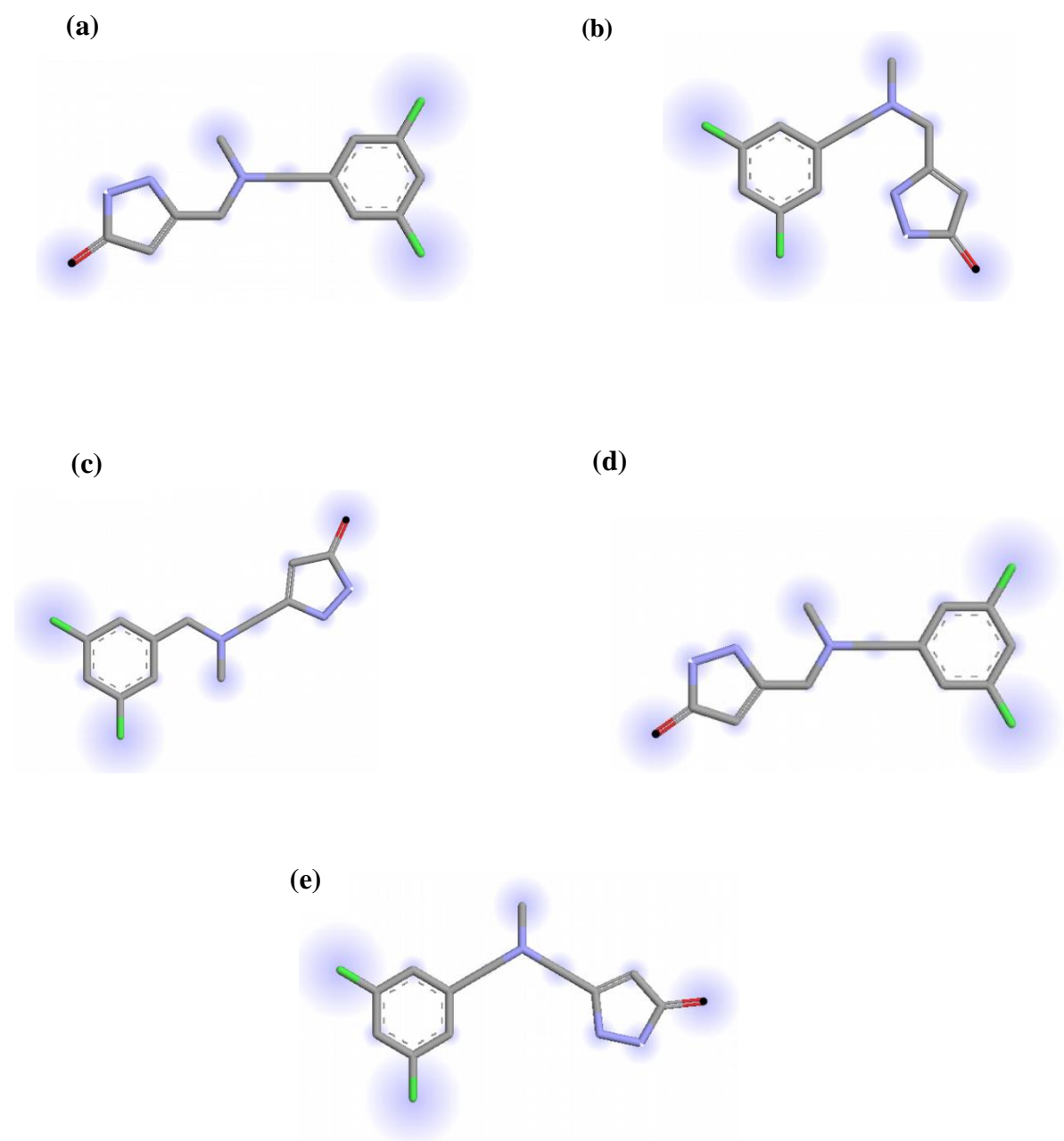
Figure S13: Snapshots of TAP bound to MT-SOD1 at the UMP binding site of SOD1 at (a) 100 ns (b) 150 ns (c)200 ns (d) 250 ns (e) 300 ns of MD simulation

(a)

(b)

(c)
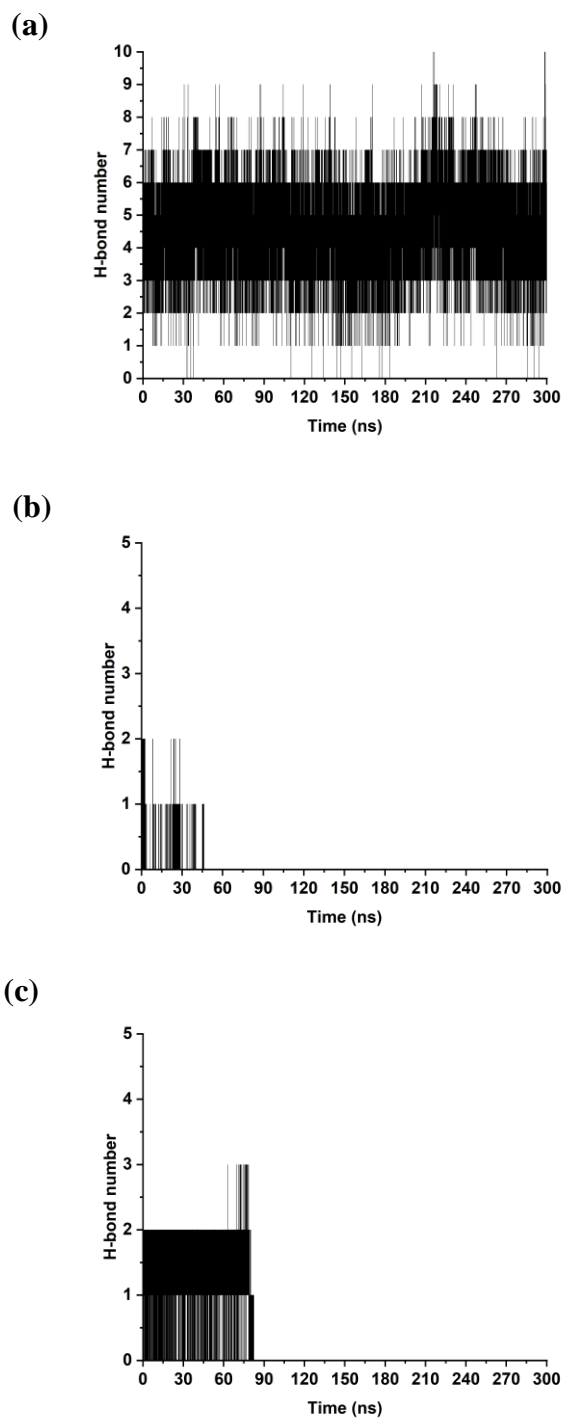
Figure S14: H-bond number in the complex MT-SOD1-TAP when the ligand is bound at (a) dimeric interface cavity (b) W32 binding site (c) UMP binding site of SOD1
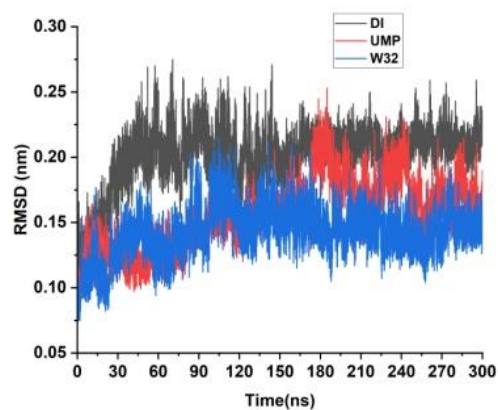
Figure S15: RMSD plot of the MT-SOD1-PCF system

(a)

(b)

(c)
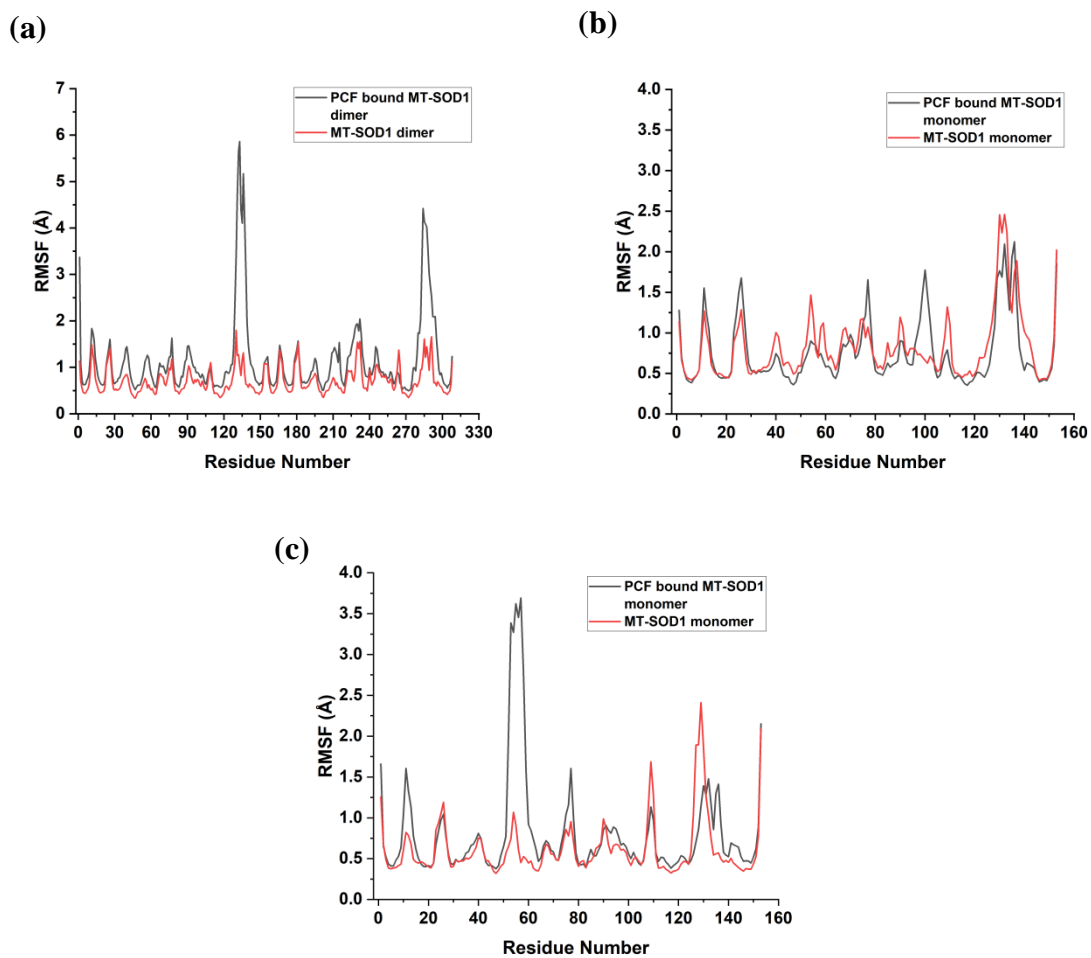
Figure S16: Plot depicting residual flexibility of the residues for PCF binding to MT-SOD1 at (a) dimeric interface cavity (b) W32 binding site **(c)** UMP binding site
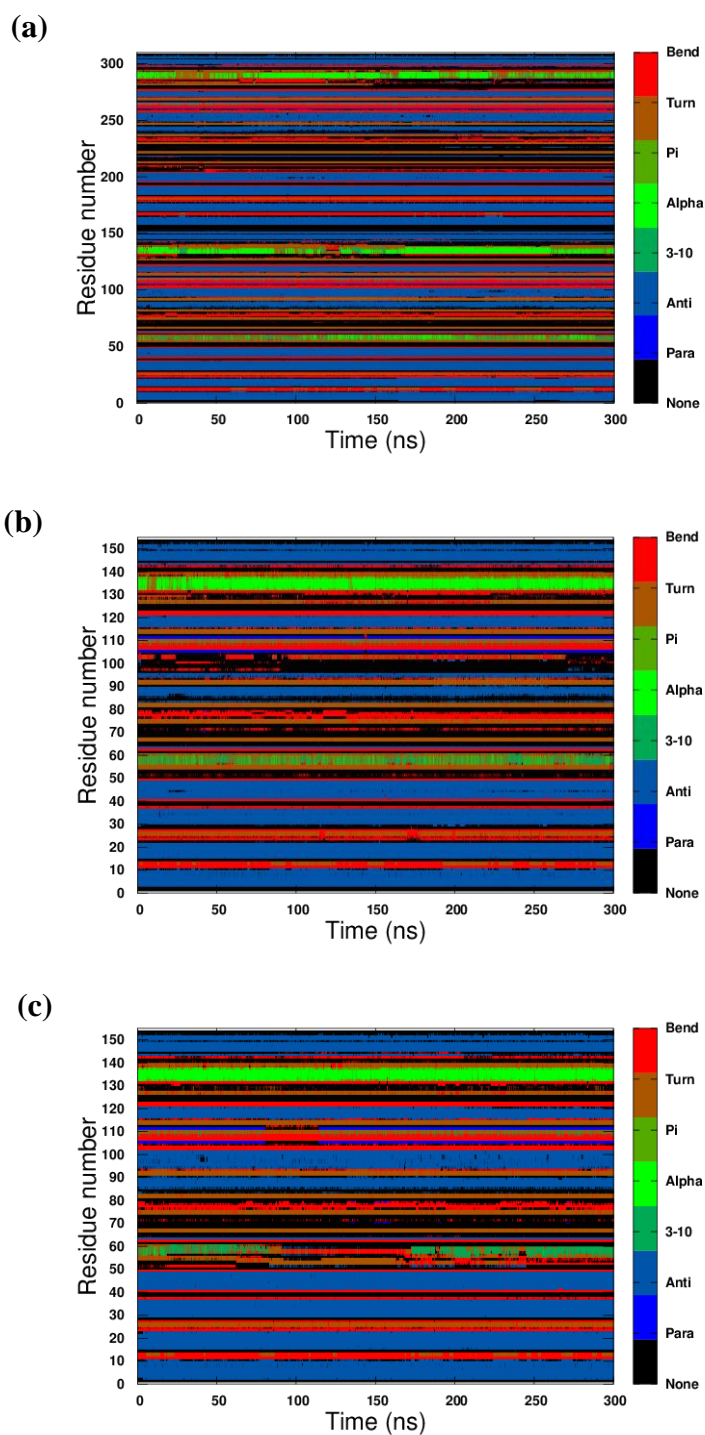
Figure S17: Secondary structure propensity analysis of the MD trajectories for PCF binding to MT-SOD1 at (a) dimeric interface cavity (b) W32 binding site **(c)** UMP binding site
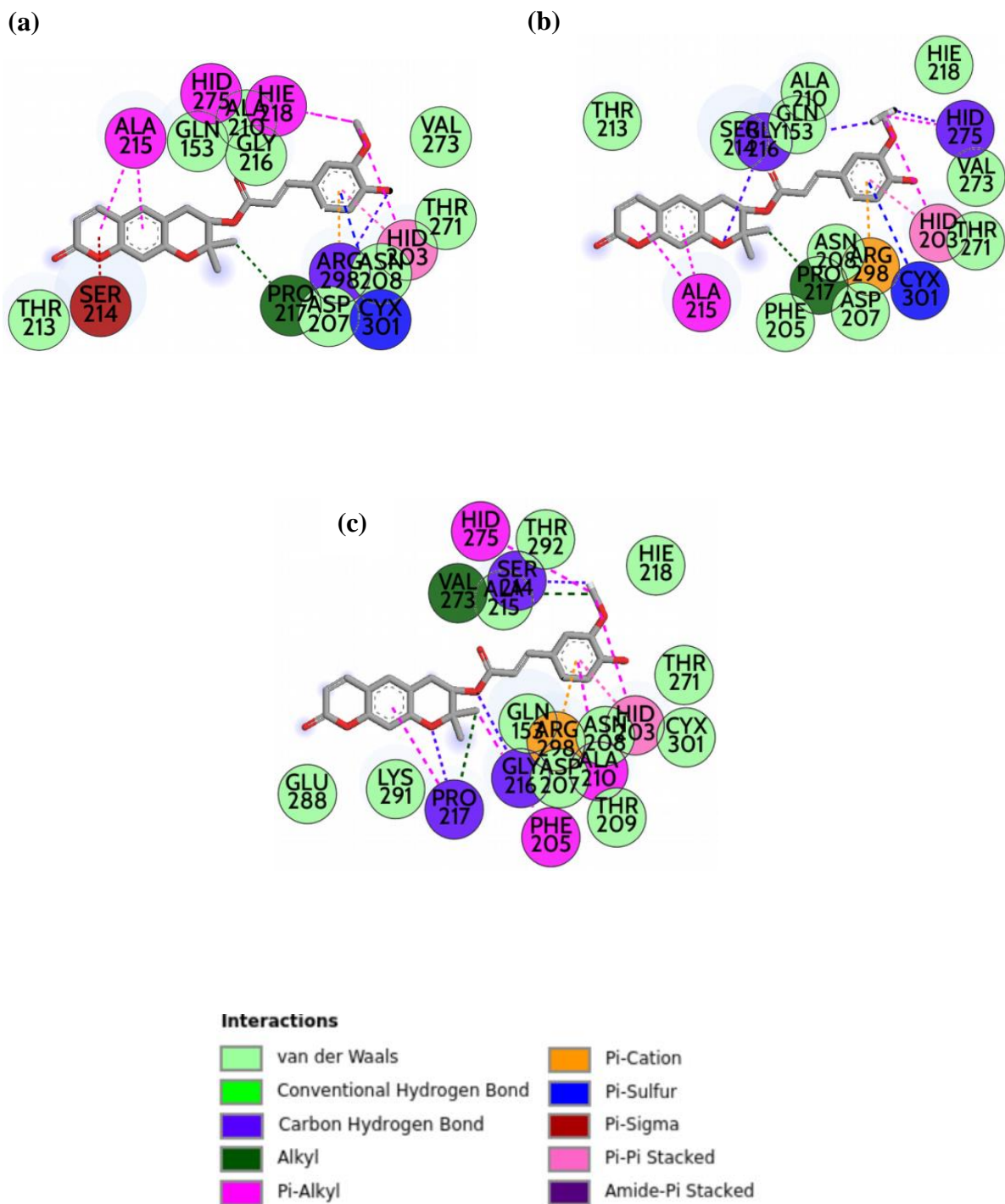
Figure S18: Snapshots of PCF bound to MT-SOD1 at the dimeric interface cavity of SOD1 at (a) 150 ns (b) 200 ns (c) 250 ns of MD simulation
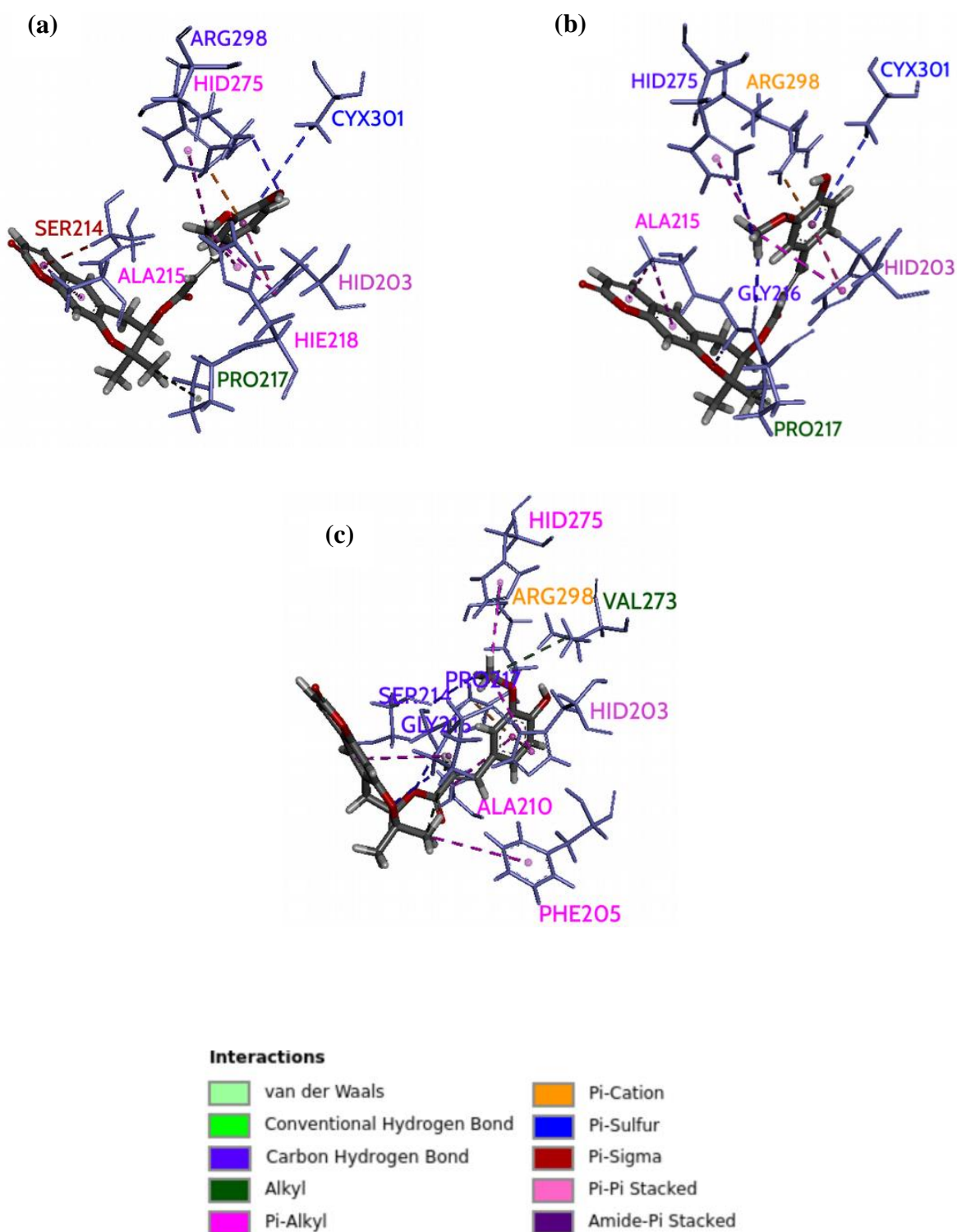
Figure S19: 3D representation of protein-ligand interactions shown by PCF bound to MT-SOD1 at the dimeric interface cavity of SOD1 at (a) 150 ns (b) 200 ns (c) 250 ns of MD simulation

Time	Interactions									
	Van der waals	Convent ional H-bond	Carbon H-bond	Alkyl	Pi-Alkyl	Pi-Cation	Pi-Sulfur	Pi-Sigma	Pi-Pi Stacke d	Amide-Pi Stacke d
100 ns	Gln153, Phe205, Asp207, Asn208, Ala210, Thr213, Ser214, Hie218, Thr271, Val273, Hid275, Thr292	-	Gly216	Pro217	Ala215, Hid203	Arg298	Cyx301	-	Hid203	-
150 ns	Gln153, Asp207, Asn208, Ala210, Thr213, Gly216, Thr271, Val273	-	Arg298	Pro217	Ala215, Hid275, Hie218,	Arg298	Cyx301	Ser214	Hid203	-
200 ns	Gln153, Phe205, Asp207, Asn208, Ala210, Thr213, Ser214, Hie218, Thr271, Val273	-	Gly216, Hid275	Pro217	Hid203, Ala215, Hid275	Arg298	Cyx301	-	Hid203	-
250 ns	Gln153, Asp207, Asn208, Thr209, Ala215, Hie218, Thr271, Glu288, Lys291,	-	Ser214, Gly216, Pro217	Pro217, Val273	Hid203, Phe205, Ala210, Pro217, Hid275,	Arg298	-	-	Hid203	-

	Thr292, Cyx301 Asn208										
300 ns	**Asp207, Asn208, Ala210, Ala215, Pro217, Hie218, Thr271, Val273, Cyx301**	**Gln153**	**Ser214, Gly216**	**-**	**Hid275**	**Arg298**	**-**	**Ser214**	**Hid203**	**Thr213**

Table S4: Various interactions shown by the PCF bound to MT-SOD1 at the dimeric interface cavity of SOD1
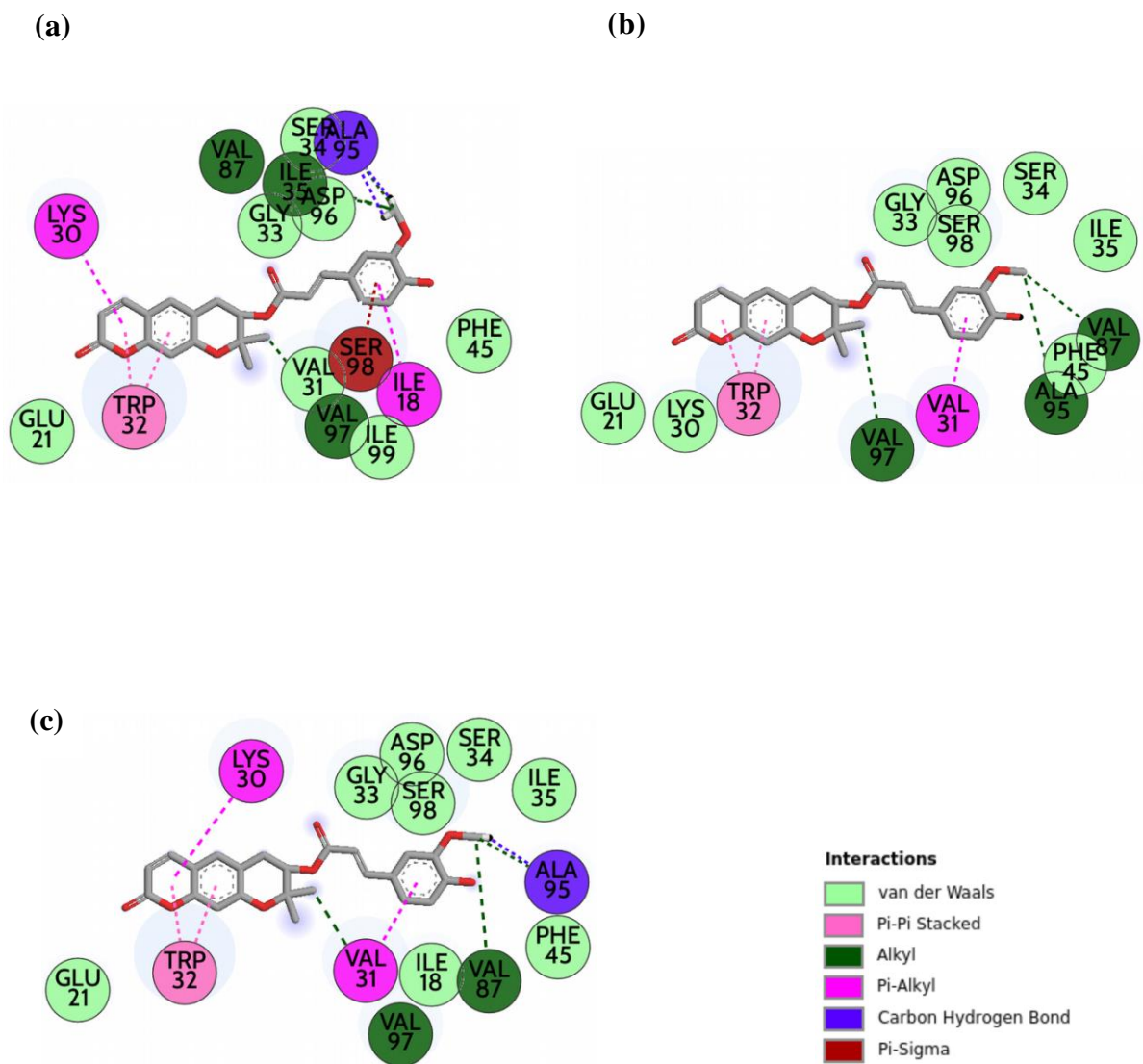
Figure S20: Snapshots of PCF bound to MT-SOD1 at the W32 binding site of SOD1 at (a) 150 ns (b) 200 ns (c) 250 ns of MD simulation

(a)

(b)

(c)

Interactions

▢	van der Waals
▢	Pi-Pi Stacked
▢	Alkyl
▢	Pi-Alkyl
▢	Carbon Hydrogen Bond
▢	Pi-Sigma
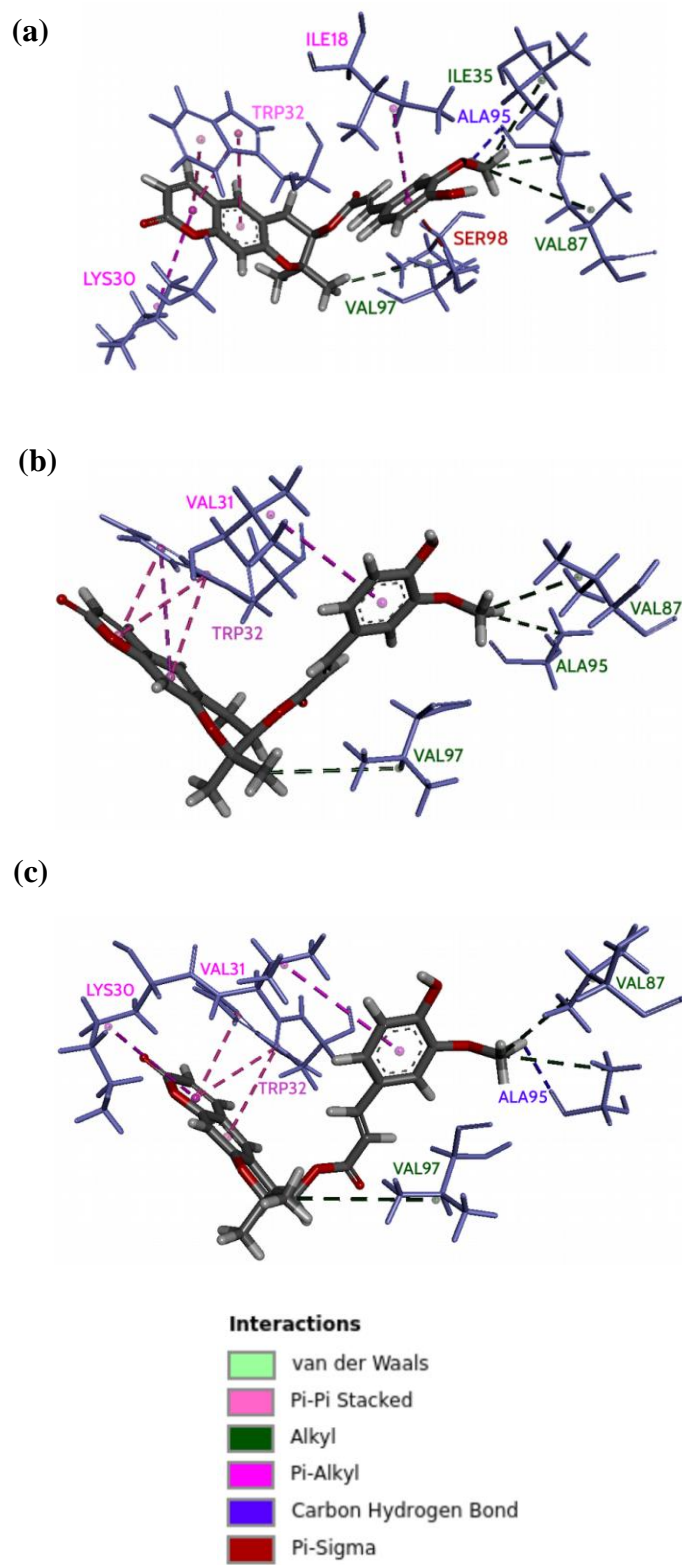
Figure S21: 3D representation of protein-ligand interactions shown by PCF bound to MT-SOD1 at the W32 binding site of SOD1 at (a) 150 ns (b) 200 ns (c) 250 ns of MD simulation

Time	Interactions					
	Van der waals	Carbon H-bond	Alkyl	Pi-Alkyl	Pi-Sigma	Pi-Pi Stacked
100 ns	Ile18, Glu21, Gly33, Ser34, Ile35, Phe45, Asp96, Ser98, Glu100	-	Val87, Val95, Val97	Lys30, Val31	-	Trp32
150 ns	Glu21, Val31, Gly33, Ser34, Phe45, Asp96, Ile99	Ala95	Ile35, Val87, Ala95, Val97	Ile18, Lys30	Ser98	Trp32
200 ns	Glu21, Lys30, Gly33, Ser34, Ile35, Phe45, Asp96, Ser98	-	Val87, Ala95, Val97	Val31,	-	Trp32
250 ns	Ile18, Glu21, Gly33, Ser34, Ile35, Phe45, Asp96, Ser98	Ala95	Val87, Ala95, Val97	Lys30, Val31	-	Trp32
300 ns	Ile18, Glu21, Lys30, Gly33, Ser34, Phe45, Val87, Asp96, Val97, Ser98	Ala95	Ile35, Ala95	Val31,	-	Trp32

Table S5: Various interactions shown by the PCF bound to MT-SOD1 at the W32 binding site of SOD1
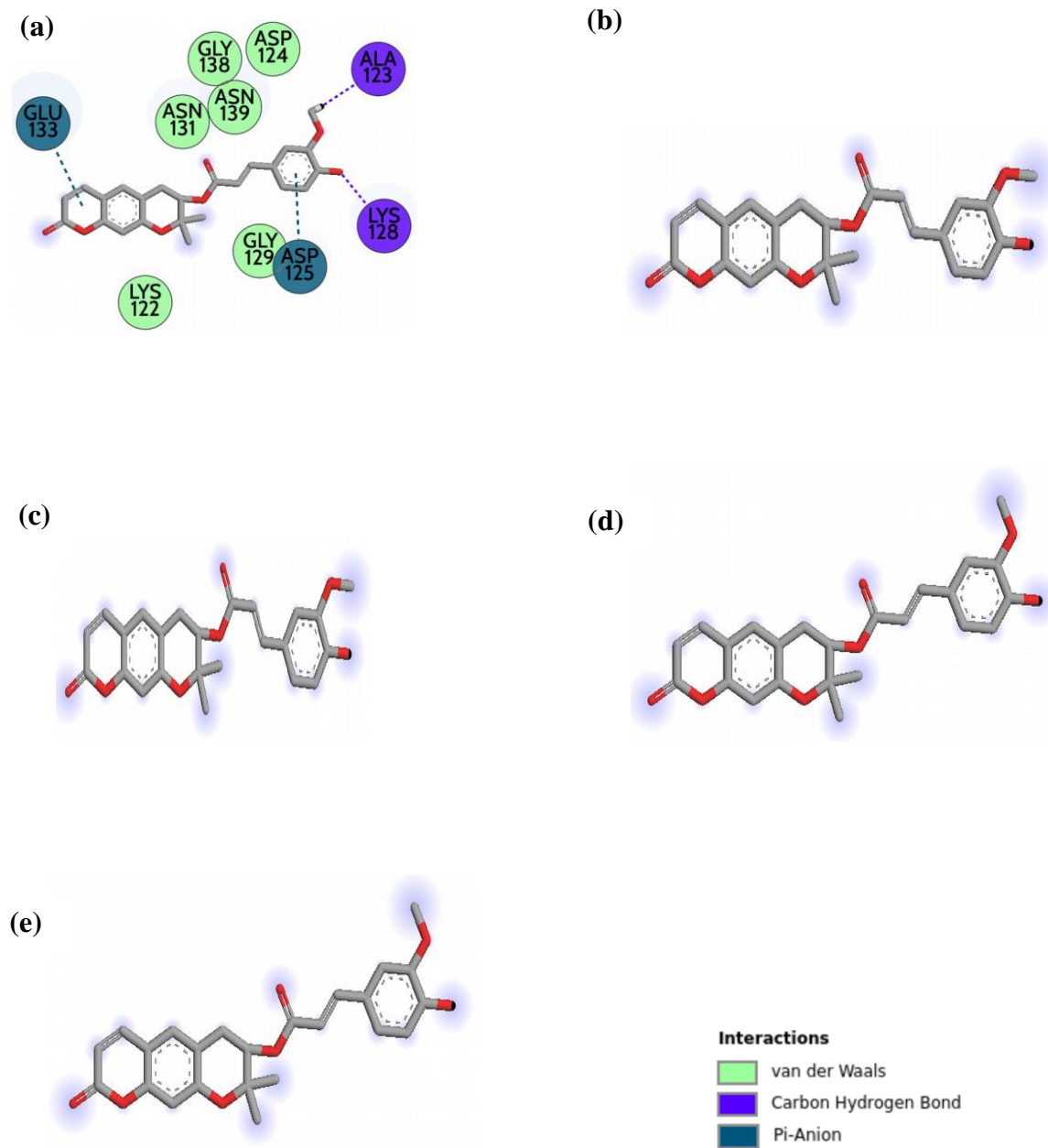
Figure S22: Snapshots of PCF bound to MT-SOD1 at the UMP binding site of SOD1 at (a) 100 ns (b) 150 ns (c) 200 ns (d) 250 ns (e) 300 ns of MD simulation
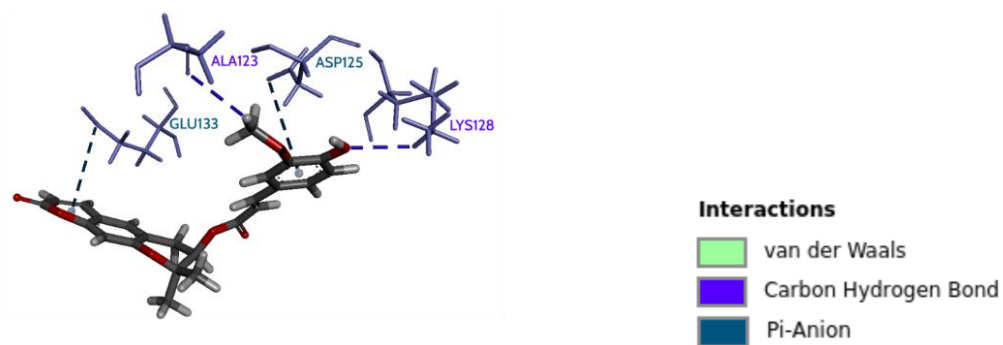
Figure S23: 3D representation of protein-ligand interactions shown by PCF bound to MT-SOD1 at the UMP binding site of SOD1 at 100 ns of MD simulation

(a)

(b)

(c)
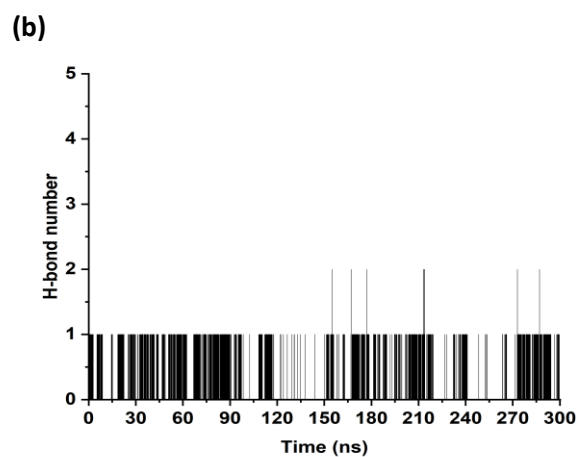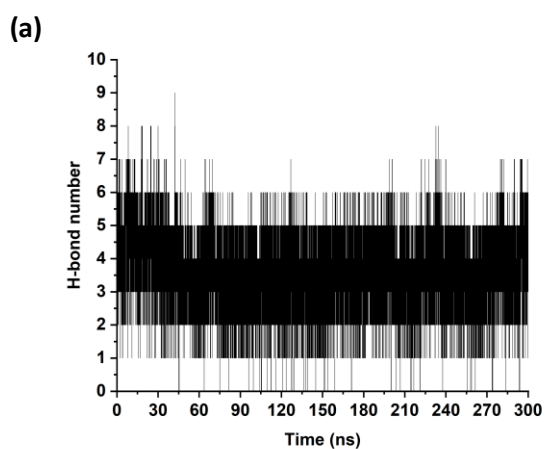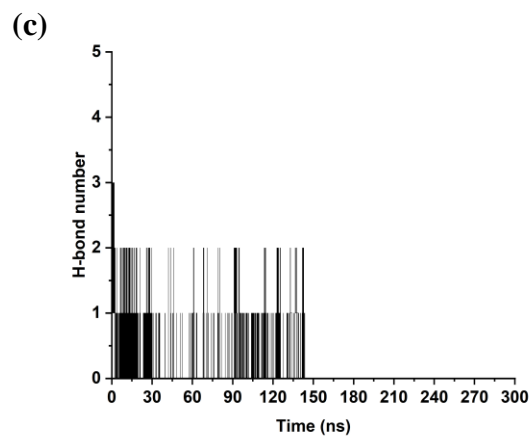
Figure S24: H-bond number in the complex MT-SOD1-PCF when the ligand is bound at (a) dimeric interface cavity (b) W32 binding site (c) UMP binding site of SOD1